Optimal Hubbard Models for Materials with Nonlocal Coulomb Interactions: Graphene, Silicene, and Benzene

M. Schüler,[1,2,*] M. Rösner,[1,2] T. O. Wehling,[1,2] A. I. Lichtenstein,[3] and M. I. Katsnelson[4]

[1]*Institut für Theoretische Physik, Universität Bremen, Otto-Hahn-Allee 1, 28359 Bremen, Germany*

[2]*Bremen Center for Computational Materials Science, Universität Bremen, Am Fallturm 1a, 28359 Bremen, Germany*

[3]*Institut für Theoretische Physik, Universität Hamburg, Jungiusstraße 9, D-20355 Hamburg, Germany*

[4]*Institute for Molecules and Materials, Radboud University of Nijmegen, Heijendaalseweg 135, 6525 AJ Nijmegen, The Netherlands*

(Received 14 February 2013; published 16 July 2013)

To understand how nonlocal Coulomb interactions affect the phase diagram of correlated electron materials, we report on a method to approximate a correlated lattice model with nonlocal interactions by an effective Hubbard model with on-site interactions U^* only. The effective model is defined by the Peierls-Feynman-Bogoliubov variational principle. We find that the local part of the interaction U is reduced according to $U^* = U - \bar{V}$, where $\bar{V}$ is a weighted average of nonlocal interactions. For graphene, silicene, and benzene we show that the nonlocal Coulomb interaction can decrease the effective local interaction by more than a factor of 2 in a wide doping range.

DOI: 10.1103/PhysRevLett.111.036601 PACS numbers: 72.80.Vp, 73.20.Hb, 73.61.Wp

Low dimensional sp-electron systems like graphene [1–3], systems of adatoms on semiconductor surfaces such as Si(111):X with X = C, Si, Sn, Pb [4], Bechgaard salts or aromatic molecules [5,6], and polymers [7,8] feature simultaneously strong local and nonlocal Coulomb interactions. In graphene, for instance, the on-site interactions $U/t \sim 3.3$, the nearest neighbor Coulomb repulsion $V/t \sim 2$, as well as further sizable nonlocal Coulomb terms exceed the nearest neighbor hopping $t = 2.8$ eV [1]. Considering on-site interactions $U/t \sim 3.3$ alone would put graphene close to the boundary of a gapped spin liquid [9], which could be even crossed by applying strain on the order of a few percent [1]. It is currently unclear whether [10] or not [11,12] nonlocal Coulomb interactions stabilize the semimetallic Dirac phase in graphene. To rephrase the problem, it is unclear which Hubbard model with strictly local interactions would yield the best approximation to the ground state of graphene. To judge the stability of the Dirac electron phase in graphene but also to understand Mott transitions on surfaces like Si:X (111), a quantitative well defined link from models with local and nonlocal Coulomb interactions to those with purely local interactions is desirable.

In this Letter, we present a method to map a generalized Hubbard model with nonlocal Coulomb interactions onto an effective Hubbard model with on-site interactions U^* only. For graphene, silicene, and benzene we show that nonlocal terms reduce the effective on-site interaction by more than a factor of 2 in a wide doping range around half filling. Thus, nonlocal Coulomb interactions are found to stabilize the Dirac electron phases in graphene and silicene against spin-liquid and antiferromagnetic phases. In the almost empty and nearly filled case we find, however, that even strictly repulsive nonlocal Coulomb interactions can effectively increase the local interactions.

The starting point is the extended Hubbard model

$$H = -\sum_{i,j,\sigma} t_{ij} c^\dagger_{i\sigma} c_{j\sigma} + U \sum_i n_{i\uparrow} n_{i\downarrow} + \frac{1}{2} \sum_{\substack{i \neq j \\ \sigma,\sigma'}} V_{ij} n_{i\sigma} n_{j\sigma'}, \quad (1)$$

where t_{ij} are the hopping matrix elements. U and V_{ij} are the local and nonlocal Coulomb matrix elements, respectively. The goal is to map the Hamiltonian (1) onto the effective model

$$H^* = -\sum_{i,j,\sigma} t_{ij} c^\dagger_{i\sigma} c_{j\sigma} + U^* \sum_i n_{i\uparrow} n_{i\downarrow}. \quad (2)$$

The effective on-site interaction U^* shall be chosen such that the canonical density operator $\rho^* = 1/Z^* e^{-\beta H^*}$ of the auxiliary system, where $Z^* = \mathrm{Tr}\{e^{-\beta H^*}\}$ is the partition function, approximates the exact density operator ρ derived from H as close as possible. This requirement leads to the Peierls-Feynman-Bogoliubov variational principle [13–15] for the functional

$$\tilde{\Phi}[\rho^*] = \Phi^* + \langle H - H^* \rangle^*, \quad (3)$$

where $\Phi^* = -(1/\beta) \ln Z^*$ is the free energy of the auxiliary system. $\langle \cdots \rangle^* = \mathrm{Tr} \rho^* (\cdots)$ denotes thermodynamic expectation values with respect to the auxiliary system. In the case of $\rho^* = \rho$ the functional $\tilde{\Phi}[\rho^*]$ becomes minimal and coincides with the free energy. The optimal U^* is thus obtained for minimal $\tilde{\Phi}[\rho^*] = \tilde{\Phi}[U^*]$:

$$\partial_{U^*} \tilde{\Phi}[U^*] = 0. \quad (4)$$

By evaluating Eq. (4) one finds

$$U^* = U + \frac{1}{2} \sum_{\substack{i \neq j \\ \sigma,\sigma'}} V_{ij} \frac{\partial_{U^*} \langle n_{i\sigma} n_{j\sigma'} \rangle^*}{\sum_l \partial_{U^*} \langle n_{l\uparrow} n_{l\downarrow} \rangle^*}. \quad (5)$$

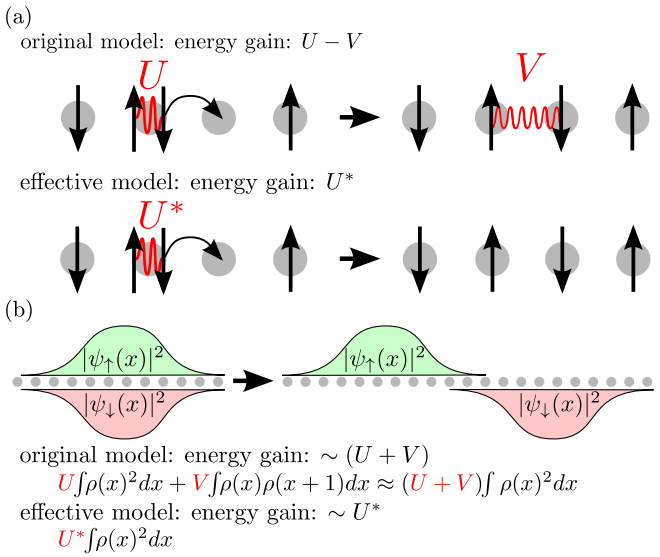

FIG. 1 (color online). Illustration of the physical process underlying Eq. (5). (a) Half-filled system: an electron hops from a doubly occupied site to an empty one, gaining an energy $(U - V)$ in the original model and U^* in the effective model. (b) Nearly empty or almost full system: wave packets of spin up and down electrons or holes $[\rho(x) = |\psi_{\uparrow,\downarrow}(x)|^2]$ are separated to the farthest possible position. If the packets are much wider than the lattice spacing, the approximation for the initial energy $U\int\rho(x)^2dx + V\int\rho(x)\rho(x+1)dx \approx (U+V)\int\rho(x)^2dx$ holds and the energy gained in the original model is $\sim(U + V)$ and $\sim U$ in the effective model.

This rule presents a central result of this Letter and has an intuitive physical interpretation (see Fig. 1): increasing the on-site term U^* reduces the double occupancy $\langle n_{i\uparrow}n_{i\downarrow}\rangle^*$ and pushes away electrons approaching an already occupied site $i = 0$ to neighboring sites. In the case of purely local Coulomb interactions there is a Coulomb energy gain of U^* upon suppressing the double occupancy. When there are, however, nonlocal Coulomb interactions with surrounding lattice sites j, the displaced electrons raise the energy of the system by terms proportional to V_{0j}. For a system at half filling with one doubly occupied site this process is illustrated in Fig. 1(a). In this case, it is obvious that the Coulomb energy gains due to the electron displacement in the original and the auxiliary model become energetically equivalent for $U^* = U - V$. We will show that this picture applies well for graphene, silicene, and benzene in a wide doping range.

For a translationally invariant system, the local part of the interaction U is reduced according to $U^* = U - \bar{V}$, where

$$\bar{V} = -\sum_{\substack{j\neq 0\\ \sigma'}} V_{0j}\frac{\partial_{U^*}\langle n_{0\uparrow}n_{j\sigma'}\rangle^*}{\partial_{U^*}\langle n_{0\uparrow}n_{0\downarrow}\rangle^*}. \quad (6)$$

The conservation of the total electron number N leads to the sum rules $\sum_{j\sigma}\langle n_{0\uparrow}n_{j\sigma}\rangle^* = N/2$ and $\partial_{U^*}\langle n_{0\uparrow}n_{0\downarrow}\rangle^* = -\sum_{j\neq 0,\sigma}\partial_{U^*}\langle n_{0\uparrow}n_{j\sigma}\rangle^*$. Thus, $\bar{V}$ is a weighted average of the nonlocal Coulomb interactions. Under the assumption that an increasing U^* displaces electrons only to next neighbors, we find $\partial_{U^*}\langle n_{0\uparrow}n_{0\downarrow}\rangle^* = -N_n\partial_{U^*}\sum_\sigma\langle n_{0\uparrow}n_{1\sigma'}\rangle^*$, where N_n is the coordination number. Equation (5) then yields

$$U^* = U - V_{01}. \quad (7)$$

This gives an estimate for the effective Coulomb interaction without the need of numerical calculations but it follows from a severe approximation. The following numerical calculations show, however, that in a wide doping range around half filling Eq. (7) leads to values close to the exact ones (shown in Table I). Then, the nonlocal Coulomb interaction reduces the effective on-site interaction and therefore stabilizes the Fermi sea against transitions, e.g., to a Mott insulator. Nevertheless, situations with negative $\bar{V}$ can be constructed, as will be demonstrated for systems with nearly empty or almost filled bands further below.

When the approximation that electrons are only displaced to next neighbors is dropped, the derivatives of the correlation functions have to be calculated explicitly. This can be done approximately within the dynamical mean field theory [17] and diagrammatic extensions like the dual-fermion approach [18]. In certain cases also numerically exact calculations of the nonlocal charge correlation functions for instance by means of exact diagonalization (ED), determinant quantum Monte Carlo (DQMC [19]) calculations, or density-matrix renormalization group methods (see, e.g., Ref. [20]) are possible.

In the following, we consider graphene, silicene, and benzene by means of DQMC calculations and ED. We used the DQMC implementation "QUantum Electron Simulation Toolbox" (QUEST 1.3.0 [21]) on a super cell to obtain the charge correlation functions that enter Eq. (5) for graphene and silicene at half filling. Furthermore, a different DQMC implementation [22] was used to verify the results of the QUEST package. The Hubbard model with less than 8–9 sites can also be solved by exact diagonalization. In this case a comparison with data obtained with

TABLE I. First three rows: Coulomb matrix elements obtained with cRPA (graphene and silicene) and from Ref. [16] for benzene ($t_{\text{graphene}} = 2.80$ eV, $t_{\text{silicene}} = 1.14$ eV, $t_{\text{benzene}} = 2.54$ eV). Last three rows: effective local Coulomb matrix elements for half filling with and without the approximation that electrons are only displaced to nearest neighbors and factor by which the local Coulomb interaction is decreased.

	Graphene	Silicene	Benzene
U/t	3.63	4.19	3.96
$(V_{01}, V_{02})/t$	2.03, 1.45	2.31, 1.72	2.83, 2.01
$(V_{03}, V_{04})/t$	1.32, 1.14	1.55, 1.42	1.80, −
U^*/t	1.6 ± 0.2	2.0 ± 0.3	1.2
$(U - V_{01})/t$	1.6	1.9	1.1
U^*/U	0.45 ± 0.05	0.46 ± 0.05	0.3

DQMC calculations shows excellent agreement (see Supplemental Material [23]).

To calculate U^* for realistic systems, we introduce values for the Coulomb interactions in the original model defined by Eq. (1). For graphene and silicene these values are calculated with the constrained random phase approximation (cRPA) [24] as in Ref. [1]. For benzene, we use values from Ref. [16], which are obtained by fitting U and t to experimental spectra and calculating V_{ij} by the Ohno interpolation [25], which reads

$$V_{ij}(\varepsilon) = \frac{U}{\sqrt{1 + (\alpha \varepsilon r_{ij})^2}} \tag{8}$$

with $\alpha = U/e^2$. The nonlocal Coulomb interaction can be tuned by an additional variable screening ε ranging from 0 to ∞. $\varepsilon = \infty$ corresponds to purely local interactions and $\varepsilon = 0$ to ultimately nonlocal interactions with matrix elements not decaying with distance between sites. $\varepsilon = 1$ corresponds to the model of benzene proposed in Ref. [16]. For all systems the values of the initial Coulomb interactions are given in Table I.

For a honeycomb lattice at half filling the U^* derivatives of the correlation functions $\partial_{U^*}\langle n_{0\uparrow} n_{j\sigma'}\rangle^*$ at $U^* = 2t$ are shown in Fig. 2(a) [26]. In this particular case, $\partial_{U^*}\langle n_{0\uparrow} n_{j\sigma'}\rangle^*$ changes sign with both sublattice and spin indices. Generally, $|\partial_{U^*}\langle n_{0\uparrow} n_{j\downarrow}\rangle^*|$ with opposite spins exceeds the equal spin case $|\partial_{U^*}\langle n_{0\uparrow} n_{j\uparrow}\rangle^*|$. The derivatives decrease clearly with the distance between the sites $i = 0$ (thick drawn circles in the middle) and j. Thus, our numerical calculations show that upon increasing U^* double occupancy is indeed reduced by displacing electrons to close by neighboring sites, and support the scenario suggested in Fig. 1(a).

The resulting values of the effective local Coulomb interaction U^* for graphene, silicene, and benzene are summarized in Table I. The local Coulomb interaction is decreased by a factor of larger than 2 in all cases. For both graphene and silicene the renormalized on-site interactions are far away from the transition to a gapped spin liquid at $U^*/t = 3.5$ [9]. The Dirac semimetal phase is thus stabilized by the nonlocal Coulomb interactions. We obtain the strongest renormalization of the on-site interaction for benzene. This is mostly due to the different ratio between local and nonlocal Coulomb interactions in benzene, $V_{01}/U = 0.72$, as compared to $V_{01}/U = 0.56$ for graphene [27] or $V_{01}/U = 0.55$ for silicene.

It is interesting to see how the renormalization of the local Coulomb interaction depends on the filling of the system. Therefore, we study the model of benzene at an arbitrary number of electrons N by means of ED. The initial Coulomb matrix elements entering Eq. (1) are assumed to be doping independent. The results for the filling dependent U^*/t in benzene for different strengths of the nonlocal Coulomb interaction $V_{ij}(\varepsilon)$ from Eq. (8) are shown in Fig. 3. Clearly doping in the range of $4 \leq N \leq 8$ has only little effect on U^*. This doping range corresponds to changing the number of electrons on the order of $\pm 1/3$ per atom and thus covers fully the range of dopings which can be achieved in graphene by means of gate voltages or adsorbates.

Strong differences to the half-filled case arise however for extreme doping ($N = 2$, 10), i.e., close to the nearly empty or almost completely filled case. The reduction of the effective local interaction U^* is considerably weaker [see Fig. 3(a)]. For a stronger initial on-site interaction ($U = 7.92t$) U^* even exceeds the initial on-site interaction by a factor of up to $U^*/U \approx 1.3$ [see Fig. 3(b)]. The physical origin of the behavior is illustrated in Fig. 1(b). In a dilute system, two electronic wave packages can minimize their Coulomb energy by simply avoiding each other in real space while staying delocalized over many lattice spacings at the same time. For such delocalized wave packages the effect of on-site and, e.g., nearest neighbor Coulomb interactions becomes very similar and the on-site interaction U^* is increased by V.

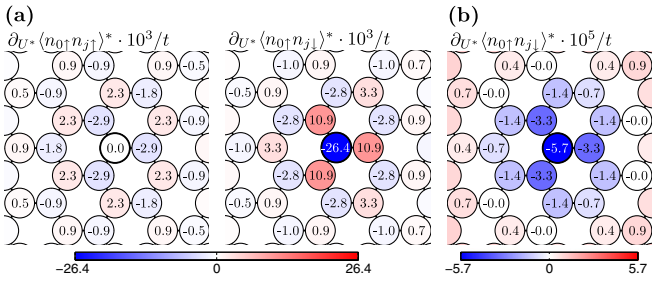

FIG. 2 (color online). (a) Derivatives of the correlation functions $\langle n_{0\uparrow} n_{j\sigma}\rangle$ with respect to U^* at $U^* = 2t$ for half-filled graphene (16×16 unit cells). Each circle corresponds to one carbon atom. The thick drawn circles indicate the lattice site with index $i = 0$. (b) Correlation function $\partial_{U^*}\langle n_{0\uparrow} n_{j\downarrow}\rangle^*$ for nearly empty honeycomb lattice (two electrons in a 5×5 super cell). In addition, we find $\partial_{U^*}\langle n_{0\uparrow} n_{j\uparrow}\rangle^* = 0$ as it must be for a singlet ground state (not shown here).

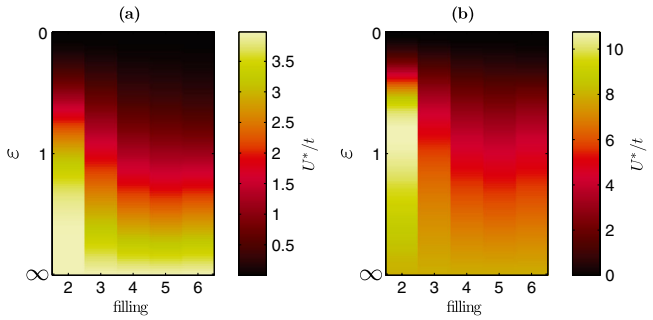

FIG. 3 (color online). Effective local Coulomb interaction U^*/t color coded for (a) benzene with $U = 3.96/t$ and (b) benzene with $U = 7.92/t$, for various screenings of $V_{ij}(\varepsilon)$ and all fillings. Due to particle hole symmetry of the model only $N \leq 6$ is shown.

This effect can be generally expected in nearly empty and almost filled systems: Fig. 2(b) shows the U^* derivatives of charge correlation functions in a 5×5 supercell of a honeycomb lattice occupied by $N = 2$ electrons in total. Most importantly, $\partial_{U^*}\langle n_{0\uparrow} n_{j\downarrow}\rangle^*$ shows pronounced differences to the half-filled case. In addition to a suppression of double occupancy by increased U^* (i.e., $\partial_{U^*}\langle n_{0\uparrow} n_{0\downarrow}\rangle^* < 0$ as in the half-filled case) $\partial_{U^*}\langle n_{0\uparrow} n_{j\downarrow}\rangle^*$ is negative in the vicinity of $j = 0$, too. Increasing local interactions with an electron at site $j = 0$ expels other electrons also from its vicinity. This corresponds to the process depicted in Fig. 1(b) and leads to effective on-site interactions being increased by nonlocal Coulomb terms. This can be understood in terms of Wigner crystallization [28]. In the full model the Coulomb energy wins over the kinetic energy for low electron or hole densities. Thus the carriers tend to localize. To approach a Wigner crystal also in the auxiliary model, the effective local interaction is increased such that interaction energy dominates over kinetic energy.

Finally, the question arises as to how accurately the effective model reflects the physical properties of the original model. The phase diagram of the extended Hubbard model on the honeycomb lattice includes an antiferromagnetic (AF), a semimetal (SM), and a charge density wave (CDW) phase [29], while the Hubbard model with strictly local interactions only features the first two phases. Similarly, if the system is in a quantum Hall regime, i.e., presence of strong magnetic fields, there are some many-body phenomena like the formation of stripes where the long-range tails of the Coulomb interaction are crucially important. In situations with such charge inhomogeneities the auxiliary model can likely fail to provide a physically correct description of the original system. If the parameters of the extended model are, however, clearly inside the AF or the SM phase, the effective model will likely approximate the physical properties of the original model quite well.

We illustrate this expectation with the example of modified benzene. In this model, the nonlocal Coulomb interaction V_{ij} are calculated with the Ohno interpolation (8). Comparisons of the spin $\langle S_z^{ij}\rangle = \langle (n_{i\uparrow} - n_{i\downarrow})(n_{j\uparrow} - n_{j\downarrow})\rangle$ and the density correlation functions $\langle \rho^{ij}\rangle = \langle (n_{i\uparrow} + n_{i\downarrow}) \times (n_{j\uparrow} + n_{j\downarrow})\rangle$ for the extended and the auxiliary local Hubbard model are shown in Fig. 4. The correlation functions have been calculated by exact diagonalization for both the original and the effective model. For $\varepsilon = 0$ and $\varepsilon \to \infty$ (noninteracting and local limit, respectively) the correlation functions of the effective and original model coincide as they should. CDW physics would manifest in $\langle \rho^{ij}\rangle$ and here we find indeed some differences of $\langle \rho^{ij}\rangle$ for the effective and the auxiliary model for intermediate screening ($\epsilon \sim 1$). However, nearly no deviation of $\langle S_z^{ij}\rangle$ between the extended and effective model is found. This behavior is found for all fillings and also different initial local interactions U (see Supplemental Material [23]).

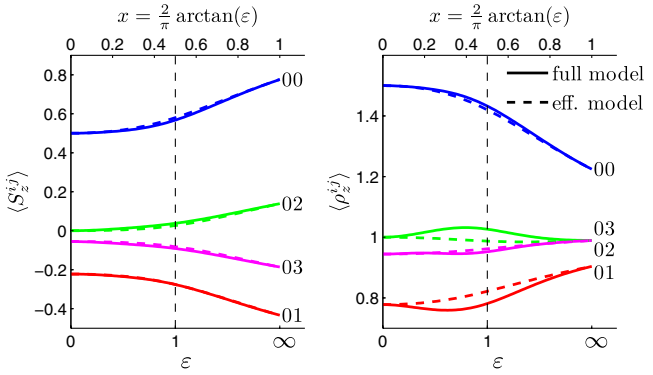

FIG. 4 (color online). Correlation as functions of the screening for the extended Hubbard model (continuous lines) and the effective Hubbard model (broken lines) for benzene. The left panel shows spin correlation $\langle S_z^{ij}\rangle$ and the right panel shows density correlation $\langle \rho_z^{ij}\rangle$. $\langle S_z^{01}\rangle$ is virtually the same for the effective and original model. The parameters for the original model are $U = 10.06$ eV and $t_{\text{orig}} = 2.539$ eV, and $V(\varepsilon)$ is calculated by Eq. (8). $U^*(\varepsilon)$ is calculated by Eq. (5), while $t_{\text{eff}} = t_{\text{orig}}$.

We thus expect that transitions into phases like an AF insulator (or a Mott insulator) will be very well described by the effective model.

In conclusion, a systematic map from lattice models with nonlocal Coulomb interactions to effective Hubbard models with strictly local Coulomb interactions U^* is derived. The physical properties of the effective model reflect the original system nicely, especially regarding spin related properties. We find that the nonlocal Coulomb interactions can significantly renormalize the effective on-site interaction U^* as compared to the original local U. In the cases of graphene and silicene our calculations yield $U^*/U < 0.5$ for half filling. Thus, the nonlocal Coulomb interactions stabilize the Dirac semimetallic phases in these materials against transitions to a gapped spin liquid or an antiferromagnetic insulator. In defective graphene or at edges local Coulomb interactions can lead to the formation of magnetic moments [3,30,31]. When describing these situations in terms of the Hubbard model, the value of $U^* = 1.6t$ obtained here should be used. Whether or not a Hubbard model is generally appropriate to describe the physical properties of graphene is still a matter of debate and depends on the observable of interest. Our results suggest that a Hubbard model should be useful to judge the occurrence of edge magnetism and of AF insulator phases. Furthermore, our work indicates that nonlocal Coulomb interactions will, in general, significantly weaken local correlation effects in sp-electron materials in a wide doping range. Additionally we have shown that for extreme low carrier densities (in the vicinity of the Wigner crystal instability) nonlocal interactions can increase the effective local interaction. Such systems should be realizable, e.g., in any weakly doped semiconductor. It is interesting to see how the renormalization of effective on-site interactions generalizes to heterostructures with modified bands and

additional van Hove singularities like twisted bilayer graphene and gated (gapped) bilayers, or to quantum Hall systems depending on Landau level filling factors.

The authors thank R. Scalletar for help with the QUEST code, F. Assaad for providing his DQMC code, and D. Mourad and F. Jahnke for helpful discussions. Financial support from DFG via SPP 1459 and FOR 1346 are acknowledged. M. I. K. acknowledges support from FOM (The Netherlands).

*mschueler@itp.uni-bremen.de

[1] T. O. Wehling, E. Şaşıoğlu, C. Friedrich, A. I. Lichtenstein, M. I. Katsnelson, and S. Blügel, Phys. Rev. Lett. **106**, 236805 (2011).
[2] V. N. Kotov, B. Uchoa, V. M. Pereira, F. Guinea, and A. H. Castro Neto, Rev. Mod. Phys. **84**, 1067 (2012).
[3] M. I. Katsnelson, *Graphene: Carbon in Two Dimensions* (Cambridge University Press, Cambridge, England, 2012).
[4] P. Hansmann, T. Ayral, L. Vaugier, P. Werner, and S. Biermann, Phys. Rev. Lett. **110**, 166401 (2013).
[5] R. Pariser and R. G. Parr, J. Chem. Phys. **21**, 767 (1953).
[6] J. A. Pople, Proc. Phys. Soc. London Sect. A **68**, 81 (1955).
[7] R. H. Friend, R. W. Glymer, A. B. Holmes, J. H. Burroughes, R. N. Marks, C. Taliani, D. D. C. Bradley, D. A. Dos Santos, J. L. Brédas, M. Lögdlund, and W. R. Salaneck, Nature (London) **397**, 121 (1999).
[8] Z. G. Soos, S. Ramasesha, and D. S. Galvão, Phys. Rev. Lett. **71**, 1609 (1993).
[9] Z. Y. Meng, T. C. Lang, S. Wessel, F. F. Assaad, and A. Muramatsu, Nature (London) **464**, 847 (2010).
[10] J. Jung and A. H. MacDonald, Phys. Rev. B **84**, 085446 (2011).
[11] C. Honerkamp, Phys. Rev. Lett. **100**, 146404 (2008).
[12] M. M. Scherer, S. Uebelacker, D. D. Scherer, and C. Honerkamp, Phys. Rev. B **86**, 155415 (2012).
[13] R. E. Peierls, Phys. Rev. **54**, 918 (1938).
[14] N. N. Bogolyubov, Dokl. Akad. Nauk SSSR **119**, 242 (1958).
[15] R. P. Feynman, *Statistical Mechanics* (Benjamin, New York, 1972).
[16] R. J. Bursill, C. Castleton, and W. Barford, Chem. Phys. Lett. **294**, 305 (1998).
[17] A. Georges, G. Kotliar, W. Krauth, and M. J. Rozenberg, Rev. Mod. Phys. **68**, 13 (1996).
[18] A. N. Rubtsov, M. I. Katsnelson, and A. I. Lichtenstein, Phys. Rev. B **77**, 033101 (2008).
[19] R. Blankenbecler, D. J. Scalapino, and R. L. Sugar, Phys. Rev. D **24**, 2278 (1981).
[20] R. M. Noack, S. R. White, and D. J. Scalapino, Phys. Rev. Lett. **73**, 882 (1994).
[21] A. Tomas, C.-C. Chang, Z.-J. Bai, and R. Scalettar, QUEST code, http://quest.ucdavis.edu/.
[22] F. F. Assaad, University of Würzburg (private communication); F. F. Assaad and H. G. Evertz, in *Computational Many Particle Physics*, Lecture Notes in Physics Vol. 739, edited by H. Fehske, R. Schneider, and A. Weiße (Springer Verlag, Berlin, 2008), p. 277.
[23] See Supplemental Material at http://link.aps.org/supplemental/10.1103/PhysRevLett.111.036601 for a discussion of the convergence with site index i of Eq. (5) and for a comparison of the spin and density correlation functions for all fillings and a different initial value for the Coulomb interaction in benzene.
[24] F. Aryasetiawan, M. Imada, A. Georges, G. Kotliar, S. Biermann, and A. I. Lichtenstein, Phys. Rev. B **70**, 195104 (2004).
[25] K. Ohno, Theor. Chim. Acta **2**, 219 (1964).
[26] DQMC calculations with 16×16 unit cells, $\beta = 9t$, $\Delta\tau = 0.05$, and 3000 measurement sweeps. To overcome the statistical noise, we fit the correlation functions with polynomials of rank 4 in U^* and evaluate the derivative analytically.
[27] A comparison with a graphene result for 8×8 unit cells, which yields the same ratio U/U^*, rules out finite size effects of the DQMC calculations.
[28] E. Wigner, Phys. Rev. **46**, 1002 (1934).
[29] I. F. Herbut, Phys. Rev. Lett. **97**, 146401 (2006).
[30] M. P. López-Sancho, F. de Juan, and M. A. H. Vozmediano, Phys. Rev. B **79**, 075413 (2009).
[31] O. V. Yazyev, Rep. Prog. Phys. **73**, 056501 (2010).